

Optics Letters

Off-axis camera-in-the-loop optimization with noise reduction strategy for high-quality hologram generation

CHUN CHEN, DONGYEON KIM, DONGHEON YOO, BYOUNGHO LEE, AND BYOUNGHO LEE*

School of Electrical and Computer Engineering, Seoul National University, Gwanak-Gu Gwanakro 1, Seoul 08826, Republic of Korea

*Corresponding author: byoungho@snu.ac.kr

Received 5 November 2021; revised 19 December 2021; accepted 19 December 2021; posted 20 December 2021; published 3 February 2022

In this Letter, we introduce a noise reduction (NR) strategy in the off-axis camera-in-the-loop (CITL) optimization for high-quality hologram generation. Our proposal adopts the Gaussian blur in the NR strategy to suppress the high-frequency noise and improve the optimization convergence. A double-hologram generation technique is used to reduce the noise further. The off-axis system's aberrations are eliminated by integrating the aberration compensation method as well. Compared with the original CITL method, the image quality of the proposed method is improved by approximately 5.5 dB in the optical experiment.

© 2022 Optica Publishing Group under the terms of the [Optica Open Access Publishing Agreement](#)

<https://doi.org/10.1364/OL.447871>

Holographic display is regarded as a promising three-dimensional display technique. It is successfully applied to augmented and virtual reality (AR/VR) displays [1–3] because it has advantages such as providing focus cues and vision correction [4–6]. Through the spatial light modulator (SLM), the hologram can reconstruct the optical wavefront of the object. As current commercial SLMs cannot modulate the amplitude and phase simultaneously, the optical wavefront needs to be encoded into either a phase-only hologram (POH) or amplitude-only hologram [7,8].

The stochastic gradient descent (SGD) method has been demonstrated to be effective in POH generation [9]. However, the reconstruction result will be affected by an imperfect optical system, such as the presence of dust and scratches on the lens and nonuniform illumination [10]. These factors can produce some noise in the reconstruction result. Recently, the camera-in-the-loop (CITL) optimization has been reported as a high-quality hologram generation method [11,12]. The CITL optimization considers the optical experiment environment, and noise in both the in-focus and out-of-focus areas can be suppressed well by adding the amplitude and phase constraints [13]. Although the noise in several systems can be reduced through the CITL optimization, the current CITL methods are mostly based on on-axis systems. Unfortunately, the on-axis systems suffer from contrast degradation because of the direct current (DC) noise from the SLM. Using the diffracted light from two SLMs to cancel the

DC noise can be a solution [12]. However, the optical system and configuration will become complicated.

Off-axis reconstruction is another way to solve the DC noise problem. By applying a linear phase ramp to the hologram [14], the diffracted light is separated from the DC component. However, severe aberrations under the off-axis reconstruction induce a gap between the physical and ideal propagation models. Because the CITL optimization method considers using the gradient information from the ideal propagation model [11], it causes gradient errors during the optimization and produces aberration noise in the reconstruction result. Furthermore, in the optical experiment environment, there are many factors that also introduce noise to the optimization process, such as the scattered light from optical devices and sensor noise. The noise affects the optimization convergence and further enlarges the gap. It is still a challenge to suppress the noise in the off-axis CITL optimization.

Here, we report an effective noise reduction (NR) method to suppress the noise in the off-axis reconstruction system based on the CITL optimization. We apply Gaussian blur to both captured raw images and simulated reconstruction images to reduce the high-frequency noise, which helps to mitigate the gap between the reconstruction results from the ideal and physical propagation model under the off-axis condition. Although applying post-processing to the captured raw image is usually considered detrimental to the CITL optimization process, we found that the Gaussian blur can be helpful for optimization convergence and image quality improvement. We also analyze the effects of the Gaussian blur on the high-frequency components and the image quality. Then, by combining the NR method with the Zernike compensation phase, the negative impact of the off-axis system's aberrations on the CITL optimization can also be eliminated. Finally, we further increase the holographic reconstruction performance by adopting the double-hologram generation strategy.

Figure 1 shows the schematic of the proposed hologram generation approach in the off-axis system. As we can see in Fig. 1, POH1 and POH2 are first added to the Zernike compensation phase to correct for the system's aberrations. Next, these two POHs are loaded onto the SLM separately. After light propagation, we can capture the temporally multiplexed holographic reconstruction results. Then, we adopt the NR method to the reconstruction result, and the loss value can be calculated by

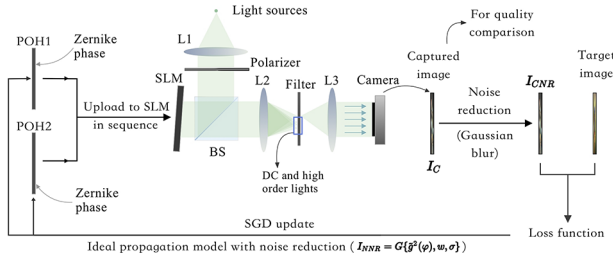


Fig. 1. Principle of the proposed method.

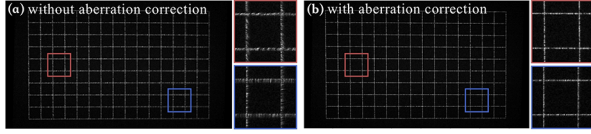


Fig. 2. Reconstructed grid patterns (a) without AC and (b) with AC.

comparing the noise-reduced image with the target image. After that, through the SGD and the ideal propagation model with NR, the double POHs can be updated based on the gradient information.

In the off-axis reconstruction system, the physical propagation model does not match well with the ideal model because of the aberrations. Thus, the gradient information for hologram updates is not accurate enough to ensure the image quality. To solve this problem, we adopt the Zernike polynomials [15, 16] as the aberration correction (AC) method. The coefficients in the Zernike compensation phase are measured through the experiment. Figures 2(a) and 2(b) show the reconstructed grid patterns without and with AC. It can be seen clearly that most of the aberrations in the system are corrected by adding the compensation phase to the hologram. The basic CITL optimization update rule with AC is given by

$$\varphi^{n+1} = \varphi^n + \varphi_z - \alpha \cdot \frac{\partial \mathcal{L}}{\partial \varphi}, \quad (1)$$

where φ is the hologram to be optimized, α is the learning rate, and \mathcal{L} is the loss function. Here, φ_z is the compensation phase which is given by $\varphi_z = \sum_i c_i Z_i$, c_i is the Zernike coefficient corresponding to the index, and Z_i is the i th Zernike polynomial. Because the gradient in the physical propagation is not accessible, $\frac{\partial \mathcal{L}}{\partial \varphi}$ can be approximately written as $\frac{\partial \mathcal{L}}{\partial g} \cdot \frac{\partial \tilde{g}}{\partial \varphi}$ [11]. Here, g is the unknown physical propagation function and \tilde{g} is the ideal propagation function. We use the angular spectrum method (ASM) [17] to model the ideal propagation, which is defined as

$$\tilde{g}(\varphi) = \mathcal{F}^{-1} \left\{ \mathcal{F} \{ u \} \cdot H(f_x, f_y) \right\},$$

$$H(f_x, f_y) = \begin{cases} e^{ikz\sqrt{1-(\lambda f_x)^2 - (\lambda f_y)^2}}, & \text{if } \sqrt{f_x^2 + f_y^2} < \frac{1}{\lambda}, \\ 0, & \text{otherwise,} \end{cases} \quad (2)$$

where u and $\tilde{g}(\varphi)$ are the complex amplitude distributions in the input and the output planes, \mathcal{F} and \mathcal{F}^{-1} represent the Fourier transform and inverse Fourier transform, respectively, $H(f_x, f_y)$ is the transfer function, k represents the wavenumber $2\pi/\lambda$, λ represents the wavelength of light, z is the propagation distance, and f_x, f_y are the spatial frequencies.

As is well known, the CITL optimization process includes a real camera. Therefore, the optimization process is easily

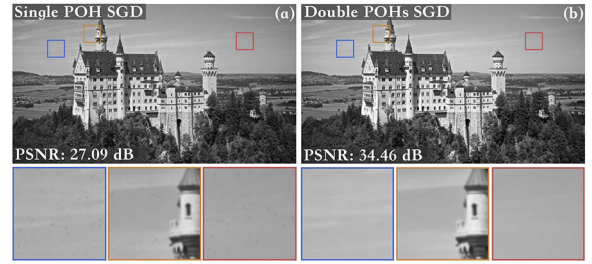


Fig. 3. Numerical reconstruction results of the (a) single-POH SGD method and (b) the proposed double-POH SGD method.

affected by many factors, such as the sensor noise and the scattered light. These factors introduce some unpredictable noise in the reconstruction results and cause the optimization process to converge to a relatively poor value. In the off-axis system, the situation is even worse because of the aberration.

To suppress the negative effects of the noise on the CITL optimization process, we propose a simple but effective NR method. First, the captured image is convolved by a Gaussian kernel with the proper kernel width w and standard deviation σ . This operation is noted by $G\{\cdot, w, \sigma\}$. Then, we have $I_{CNR} = G\{I_C, w, \sigma\}$, where I_C and I_{CNR} are the intensities of the captured image and the noise-reduced image, respectively. Second, the numerically propagated result should also apply NR in the same way. This is to guarantee the correctness of the gradient during the optimization.

$$I_{NNR} = G\{\tilde{g}^2(\varphi), w, \sigma\}, \quad (3)$$

where I_{NNR} is the numerical reconstructed intensity after the NR operation. Interestingly, instead of degrading the reconstruction image quality, our method can increase the clarity and reduce the noise in the reconstructed image under a proper blur parameter. Based on the proposed NR scheme, the optimization process is able to converge to a better value, and the high-frequency noise in the reconstruction result can be suppressed.

Moreover, we use the double-POH generation method to improve the image quality further. First, the ASM is adopted to obtain the temporally multiplexed result of the double POHs. Then, the loss function is obtained by comparing the temporally multiplexed result with the target image. Finally, the double holograms can be updated based on the SGD and the same loss function. Figure 3 shows the simulation results of the single-POH generation method and the proposed double-POH generation method. It can be seen clearly that the proposed double-hologram generation method has a clear advantage in image quality improvement.

The basic update rules of the proposed hologram generation method in Fig. 1 can be summarized as follows:

$$\varphi_1^{n+1} = \varphi_1^n + \varphi_z - \alpha \cdot \left(\frac{\partial \mathcal{L}}{\partial g_{sum}} \cdot \frac{\partial \tilde{g}_{sum}}{\partial \varphi_1} \right), \quad (4)$$

$$\varphi_2^{n+1} = \varphi_2^n + \varphi_z - \alpha \cdot \left(\frac{\partial \mathcal{L}}{\partial g_{sum}} \cdot \frac{\partial \tilde{g}_{sum}}{\partial \varphi_2} \right), \quad (5)$$

$$\tilde{g}_{sum} = \sqrt{G\{(g_1^2(\varphi_1^n) + g_2^2(\varphi_2^n))/2, w, \sigma\}}, \quad (6)$$

$$\mathcal{L}(s \cdot \tilde{g}_{sum}, a_{target}), \quad (7)$$

where φ_1 and φ_2 are the generated double POHs. We use the mean squared error as the loss function \mathcal{L} , \tilde{g}_{sum} and g_{sum} represent the amplitude of the simulated and the captured multiplexed

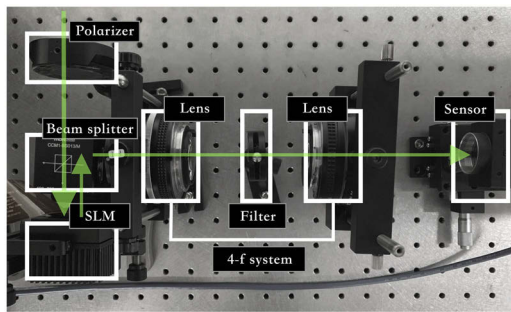


Fig. 4. Prototype of the off-axis optical reconstruction system.

reconstruction results, respectively, s is a learnable scale factor, and a_{target} is the amplitude of the target image. In the CITL optimization process, the amplitude of \tilde{g}_{sum} is replaced by that of g_{sum} , but the gradient is kept the same during the back-propagation. Through the proposed NR method, the generated holograms are able to eliminate the aberrations and reduce the noise significantly.

We implement a prototype for the holographic display experiment, as shown in Fig. 4. The phase-only SLM is provided by the Holoeye company. The pixel pitch and resolution of the SLM are $3.74 \mu\text{m}$ and 3840×2160 , respectively. The frame rate and the phase modulation range of the SLM are 60 Hz and $[0, 2\pi]$, respectively. The wavelength of the input light source is 532.0 nm. The $4f$ filter system is adopted to remove the DC and high-diffraction orders, and the camera lenses are both 50.0 mm. The propagation distance z is set to 0.12 m in our setup. The resolution of the test image is 3200×1800 px, padded with zeros out to 3840×2160 px. PyTorch 1.8.0 and Python 3.6.9 are used in the experiments to achieve the CITL optimization. The Adam optimizer [18] is adopted in the optimization, and the learning rate uses an exponential decay schedule. The central processing unit (CPU) and graphics processing unit (GPU) used in the experiments are Intel Xeon CPU @ 2.20 GHz and GTX1660 Super 6 GB with CUDA version 10.1, respectively. We use a commercial machine vision charge-coupled device (CCD) sensor (FLIR; GS3-U3-120S6M) to capture the reconstructed images. To evaluate the image quality of the reconstruction results, we adopt the peak signal-to-noise ratio (PSNR) and the speckle contrast C as criteria. Note that our approach does not apply post-processing to the final captured image for image quality measurement except for the crop operation.

Figure 5 shows the results of the SGD method, traditional CITL method, CITL method with AC method, the proposed NR method with single POH, and the proposed NR method with double POHs. The speckle contrast C is calculated inside the purple boxes, where a smaller value indicates a lower speckle noise level. Figure 5(a) shows the ground truth image. The image quality in the SGD method is quite low because there is no consideration for the experimental environment, as shown in Fig. 5(b). After the CITL optimization, some noise can be suppressed well. While the inaccurate propagation model obstructs the optimization process, the reconstructed image quality suffers from the aberrations, as shown in Fig. 5(c). With the AC, the CITL optimization can reach a lower aberration status, whereas the system's noise heavily affects the optimization process, the reconstructed details are contaminated by the speckle noise, and the artifacts caused by the Zernike compensation phase are still noticeable in the sky region, as shown in Fig. 5(d). Figure 5(e)



Fig. 5. Experimental results. (a) Ground truth image. Results of the (b) SGD, (c) CITL, (d) CITL with AC, (e) the proposed NR method with single POH, and (f) the proposed NR method with double POHs.

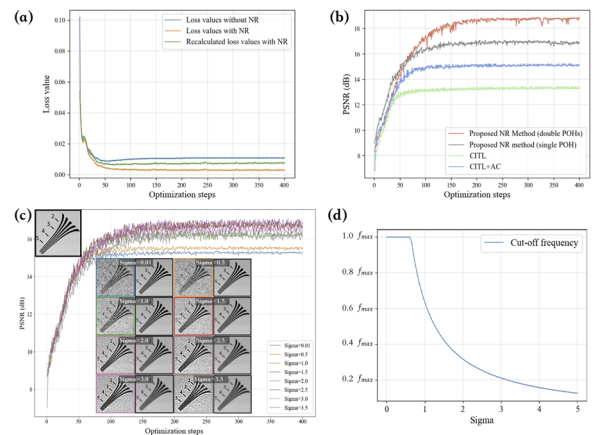


Fig. 6. (a) Loss values of the CITL with the AC method and the proposed NR method with single POH. (b) PSNR curves of the CITL method (third line from top), the CITL with AC method (bottom line), the proposed NR method with single POH (second line from top), and the proposed NR method with double POHs (top line). (c) PSNR values and reconstruction details of the proposed NR method with single POH when using different σ . (d) Relationship between the cut-off frequency of the Gaussian blur and the σ .

shows the reconstruction result of the proposed NR method with a single POH. It can be seen clearly that the NR operation is effective in the CITL optimization, and the details are revealed from the noise. Figure 5(f) is the reconstructed result of the proposed NR method with double POHs, and it shows a distinct image quality improvement compared with the previous methods. Although some noise remains in the reconstructed image

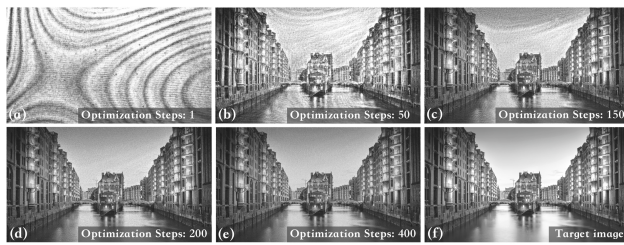


Fig. 7. Target image and evolution of the captured results using the proposed NR method with double POHs at different optimization steps, as shown in (a)–(f) (Visualization 1).

because the optical optimization experiment is imperfect, our method still achieves the highest image quality. In Fig. 6(a), the blue and orange curves represent the loss values of the CITL with the AC method and the proposed NR method with single POH, respectively. It can be seen clearly that the loss function can converge to a smaller value after the NR. However, the loss value calculated from the proposed NR method cannot completely reflect the image quality because the Gaussian blur is added to the captured raw image. Thus, to find a loss value that can better reflect the quality of the captured raw image, we recalculate the loss value by comparing the captured raw image with the target image in the proposed NR method. The green curve in Fig. 6(a) shows the recalculated loss values. Interestingly, the loss value curve also indicates a better convergence, which means a better solution is found compared with no NR operation. This is a little counter-intuitive. Using post-processing to the captured image is usually considered harmful to the CITL optimization because the real information is changed. There is a reasonable explanation for the NR operation. As we know, high-frequency noise such as speckle noise can reduce the clarity and contaminate the high-frequency contents of the reconstructed image. Because the Gaussian blur operation can be regarded as a low-pass filter, it can be used to reduce the noise [19], and thereby the negative effect of the noise on the optimization can be suppressed. Figure 6(b) shows the relationship between the PSNR and the optimization step. The curves in Fig. 6(b) also demonstrate that the proposed NR method can obtain a better convergence ability and image quality. We can see that the proposed NR method has a clear advantage in quality improvement during the optimization process. Figure 6(c) shows the relationship between PSNR values and the optimization steps when using different σ in the NR method. The test image is shown in Fig. 5(a) with a resolution ruler inside. The color boxes and black boxes in Fig. 6(c) show the influence of σ on the different frequency components at the reconstructed image and the test image. At first, when the value of σ increases, the PSNR values are improved, and the image details gradually appear. However, when σ continues to increase, the image quality is degraded, and the details are gradually blurred because some high-frequency components are lost owing to NR. The blur level of the reconstructed image is similar to that of the test image. Based on our experiments, the value of σ set to 1.5 is usually sufficient to eliminate most of the noise and keeps the image details well. Figure 6(d) shows the relationship between the approximate cut-off frequency of the Gaussian blur and σ , where f_{max} represents the ideal maximum spatial frequency of the reconstructed image. From Fig. 6(d), we can see the loss of the high-frequency components in the reconstructed result when adopting different σ . Figure 7 shows the evolution of

the captured images using the proposed NR method with double POHs. During the optimization, the captured image gradually approaches the target image.

In conclusion, we have presented a high-quality hologram generation technique under the off-axis reconstruction condition. Our method includes the NR and AC strategies, which considerably increase the image quality compared with the traditional CITL method. We demonstrate that appropriate post-processing can be used to improve the CITL optimization. The proposed NR method successfully suppresses the detrimental influence of the system's noise and provides a better convergence ability and image quality. Furthermore, by combining the NR method with the double-POH generation strategy, the image quality is improved further, because noise commonly exists in both off-axis and on-axis systems, the proposed NR method could also be extended to the on-axis system. We believe that our method has the potential to be applied to high-quality AR/VR displays.

Funding. National Research Foundation of Korea (2020K2A9A2A06038623).

Acknowledgments. This work was supported under the framework of international cooperation program managed by the National Research Foundation of Korea (2020K2A9A2A06038623).

Disclosures. The authors declare no conflicts of interest.

Data availability. Data underlying the results presented in this paper are not publicly available at this time but may be obtained from the authors upon reasonable request.

REFERENCES

- C. Jang, K. Bang, G. Li, and B. Lee, *ACM Trans. Graph.* **37**, 195 (2018).
- L. Shi, F.-C. Huang, W. Lopes, W. Matusik, and D. Luebke, *ACM Trans. Graph.* **36**, 236 (2017).
- A. Maimone, A. Georgiou, and J. S. Kollin, *ACM Trans. Graph.* **36**, 85 (2017).
- F. Yaraş, H. Kang, and L. Onural, *J. Display Technol.* **6**, 443 (2010).
- J. Hong, Y. Kim, H.-J. Choi, J. Hahn, J.-H. Park, H. Kim, S.-W. Min, N. Chen, and B. Lee, *Appl. Opt.* **50**, H87 (2011).
- C. Chang, K. Bang, G. Wetzstein, B. Lee, and L. Gao, *Optica* **7**, 1563 (2020).
- D. Yoo, Y. Jo, S.-W. Nam, C. Chen, and B. Lee, *Opt. Lett.* **46**, 4769 (2021).
- H. Dammann and K. Görtler, *Opt. Commun.* **3**, 312 (1971).
- C. Chen, B. Lee, N.-N. Li, M. Chae, D. Wang, Q.-H. Wang, and B. Lee, *Opt. Express* **29**, 15089 (2021).
- P. Chakravarthula, E. Tseng, T. Srivastava, H. Fuchs, and F. Heide, *ACM Trans. Graph.* **39**, 186 (2020).
- Y. Peng, S. Choi, N. Padmanaban, and G. Wetzstein, *ACM Trans. Graph.* **39**, 185 (2020).
- S. Choi, J. Kim, Y. Peng, and G. Wetzstein, *Optica* **8**, 143 (2021).
- S. Choi, M. Gopakumar, Y. Peng, J. Kim, and G. Wetzstein, *ACM Trans. Graph.* **40**, 240 (2021).
- H. Zhang, J. Xie, J. Liu, and Y. Wang, *Appl. Opt.* **48**, 5834 (2009).
- B. Lee, D. Yoo, J. Jeong, S. Lee, D. Lee, and B. Lee, *Opt. Lett.* **45**, 2148 (2020).
- D. Kim, S.-W. Nam, K. Bang, B. Lee, S. Lee, Y. Jeong, J.-M. Seo, and B. Lee, *Biomed. Opt. Express* **12**, 5179 (2021).
- K. Matsushima and T. Shimobaba, *Opt. Express* **17**, 19662 (2009).
- D. P. Kingma and J. Ba, Adam: a method for stochastic optimization, arXiv:1412.6980 (2014).
- E. S. Gedraite and M. Hadad, in *Proceedings ELMAR-2011*, (2011), pp. 393–396.